Acta Mineralogica-Petrographica, Szeged, XXXVII, 51–74, 1996

ALTERATION PATTERNS IN THE UMM RUS GOLD MINE AREA, EASTERN DESERT, EGYPT

NADI A. SAAD; AHMED M. EL-BOUSEILY and KHALIL I. KHALIL*

Department of Geology, Faculty of Science, Alexandria University

ABSTRACT

Mineralogical studies reveal that the common alteration minerals in the Umm Rus gold mine are chlorite, epidote, sericite and carbonates. The carbonates are mainly calcite and ankerite. Sulphidization is a common process, while silicification is the most intensive alteration process in the study area. Four alteration zones are encountered; chlorite-epidote, sericite-chlorite, sericite-ankerite-chlorite-sulphides and quartz-carbonates-sulphides zones. The textural relationship between the alteration minerals indicate that chlorite and epidote were formed firstly, followed by sericite and then by ankerite and sulphides. All the studied mineral phases were affected by silicification. The distribution of the studied alteration phases indicates that the affecting hydrothermal solutions were enriched in H_2O and CO_2 in different proportions. Elements such as K, S, As, Zn, Pb, Cu and Au are added to the system during the alteration events.

On the basis of the combined geological, mineralogical and geochemical data, four alteration stages are envisaged:

a) The hydrothermal fluids invaded the rocks through N-S shear zones. At the beginning, these fluids were characterized by low CO_2/H_2O ratio which enhanced the alteration of the biotite to chlorite and epidote. The geothermometry of the studied chlorite proves a temperature of formation of about 225°C.

b) The fluids then, became enriched in K after the breakdown of biotite. These fluids reacted with feldspars to form sericite.

c) After the formation of chlorite, epidote and sericite, the CO_2/H_2O ratio in the fluids became high and consequently ankerite was originated during this stage. Also, sulphides were concomitant with conspicuous concentration of Fe, As, Cu and Au.

d) The last stage is characterized by a severe silicification of the previously formed minerals and the formation of quartz veins. All the preceeding stages were affected by this silicification. The SiO_2-rich solution most probably remobilized the gold from sulphides (pyrrhotite) in the gabbroic rocks adjacent the granodiorite and then redistributed this gold in some other sulphide phases e. g. pyrite and pyrrhotite forming during stage c.

INTRODUCTION

More than 95 gold localities (deposits and occurrences) are known in the Eastern Desert of Egypt (EL-RAMLY et al. 1970). The Umm Rus area, the subject of this paper, is one of the largest gold mines in Egypt. It lies in the central part of the Eastern Desert, at the intersection of latitude 25° 27' 56" N and longitude 34°34'47" E (*Fig. 1*).

Gold deposit in the Umm Rus area was mined since ancient time. At the begining of twentieth century, the deposit was mined by several companies and produced about 10.000 tons of the ore (HUME, 1937 and AMIN, 1955). In the 1937 and 1938, the deposit was inspected by the Egyptian Geological Survey and the ore reserves were estimated to be

---

* Alexandria, El-Shatby. 21526, Egypt

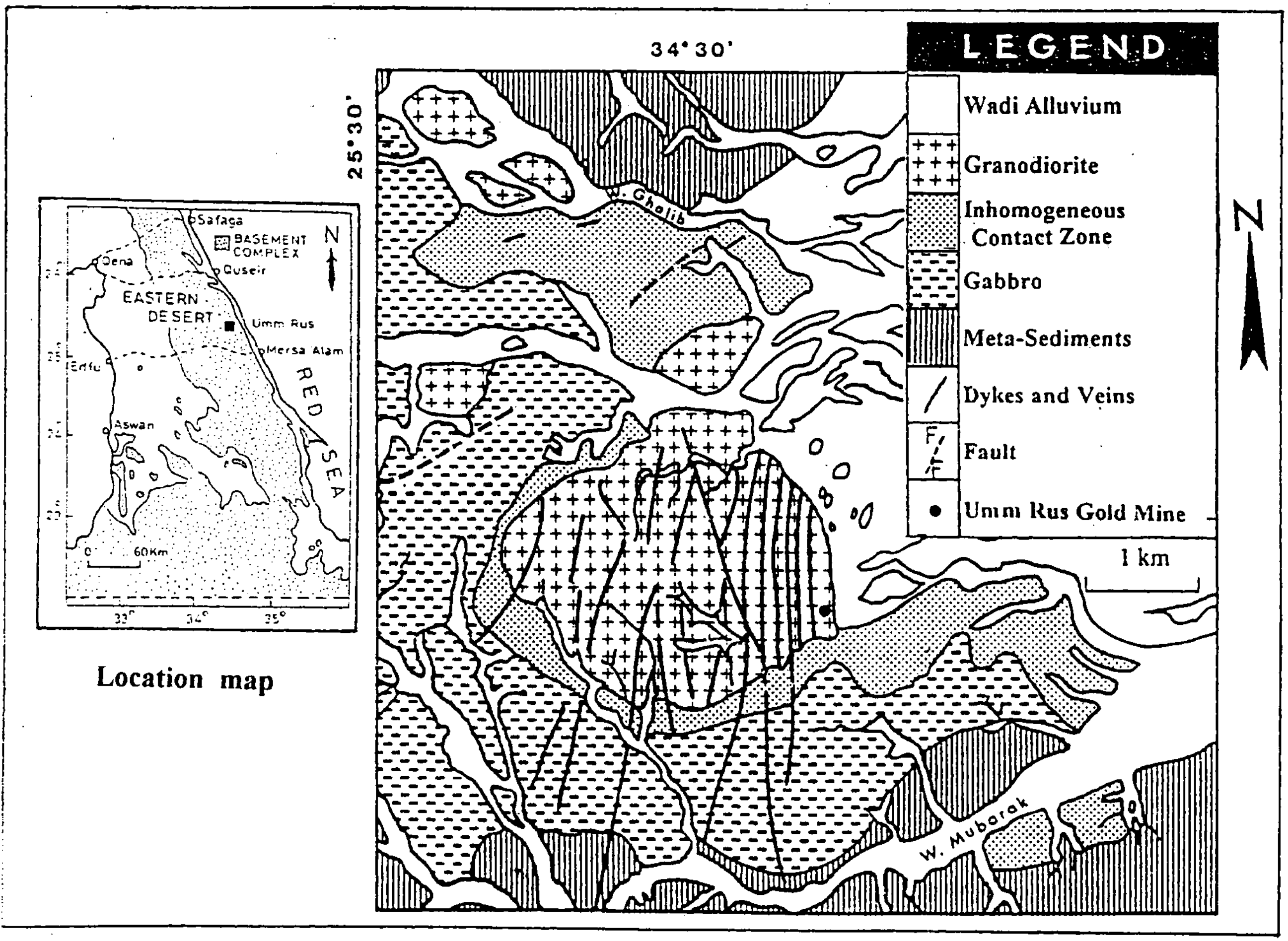

Fig. 1. Geology map of the Umm Rus area (after EL-MAHALLAWI 1984)

about 10.300 tons averaging 11,93 g/t Au (SABET, 1961). In 1940 another expedition defined additional 5800.00 tons of ore with an average of 10.85 g/t Au. During 1943–1946, the same expedition recorded 9370.00 tons of the ore. Some surface samples which were collected by the Egyptian Geological Survey during the 1968–1969 contain 27.2 g/t Au on the average. There is no information about mining activities carried out after 1969.

Field sampling for the present study (175 surface and 64 subsurface samples) was carried out to cover different rock types and quartz veins in the study area. Special attention was taken to the different alteration zones around the quartz veins. The surface sampling was carried out along profiles crossing mineralized and shear zones. Length of profiles and sampling intervals depended on ore localization and the thickness of the alteration zones. However, the subsurface samples were collected at two different depths.

A total of 115 thin and 68 polished sections were prepared for microscopic study, and results were confirmed by XRD particularly for the altered samples. Thirty polished-thin sections were microscopically selected and prepared for microprobe analysis of silicates and carbonates at the Geochemisches Institut (Göttingen University) using ARL-SEMQ-II electron microprobe equipped with six spectrometers and five different crystals (LiF, PET, ADP, TAP, PbSD). Matrix correction of the intensity measurements is made using the BENCE and ALBEE correction programme (1968). For the purpose of whole rock chemical analysis, a total of 30 samples were analyzed using a Philips PWI 408 XRF at the Geochemisches Institut, Göttingen University. The specific details of analytical precision and accuracy are given in HARTMANN and WEDEPOHL (1993).

Alteration zones in the Umm Rus area were examined by many authors as KAMEL et al. (1992) and HARRAZ and EL-DAHHAR (1994). The current study is carried out to fulfil the petrographical, mineralogical and geochemical characters of the different alteration zones, the nature of the mineralized fluids and to formulate the paragenetic sequence and the genetic model of the alteration processes.

GEOLOGIC SETTING

The Umm Rus area is covered by different rock types namely metasediments, serpentinites and related rocks, gabbros and granodiorites. The area is traversed by many quartz veins and dykes particularly in the central and southern parts of the area (*Fig. 1*).

The metasediments appear to be the oldest rock unit exposed in the area. They are regarded by KABESH et al. (1967) as typical geosynclinal sediments. The serpentinites and related rocks are presented by small exposures localized to the west and southwest of the Umm Rus area (out of the map of *Fig. 1*). The gabbro belongs to the younger ones of the Egyptian basement (TAKLA 1971) are represented by a wide exposure around the granodiorite pluton. They stratigraphically overlie the metasediments and cut across their foliation planes. The granodiorite pluton occurs as a semicircular body (ca. 7 km^2); occupiing the middle part of the area. Along the contact between the granodiorite and gabbro, a transitional heterogeneous zone mainly formed of metadiorite and metagabbro is recorded (*Fig. 1*). The granodiorite and the gabbro are traversed by several dykes and many quartz veins (*Fig. 1*). The dykes vary in composition from acidic, intermediate to basic types.

The Umm Rus gold mine area was affected by tectonism as manifested by the occurrence of numerous joints and subordinate faults particularly around the mine. The joints are of three main directions NE, NW and due E. The main fault in the investigated area extends for more than 200 m in the NE along the contact between the gabbro and the metasediments.

More than twenty different quartz veins are occurred in the Umm Rus gold mine area. Two main trends are recognized, the dominant one has a N-S direction, while the second trend has a N-NE one. Generally, the veins dip to the W and SW with an average angle of about 30°. The main lode occurs at the southeastern corner of the Umm Rus granodiorite pluton extending for more than 200 m along the quartz vein strike and reaches more than 80 m down dip. The thickness of this vein does not exceed 40 cm.

PETROCHEMISTRY

The Umm Rus granodiorite is almost fresh, and it composed of plagioclase and potash-feldspars, hornblende and biotite. The microprobe analysis of these minerals are tabulated in Tables (1–4). Plagioclase composition ranges from albite to oligoclase. Some plagioclase crystals contain a minor amount of K (orthoclase molecule, Or) up to 2.84 mol% (Table 1). The K-feldspars normally contain a small amount of albite (Ab) and anorthite (An) in solid solution. They reach up to 3.13% and 3.29%, respectively (Table 2). Biotite is a common mineral in the present granodiorite. On the Al^{IV} versus $Fe^{+2}/(Fe^{+2}+Mg)$ binary diagram of *Figure 2*, all analyses fall in the biotite field. It can be seen from Table 3 that the sum of elements occuping the K-site is less than 1.00 mol%. The deficiency is commonly compensated by the introduction of H_2O. Biotite containing water of this nature may be classified as hydrobiotite, a term first introduced by STRUNZ (1966). The type of amphiboles present in the granodiorite of the Umm Rus area is generally ferrohornblende type, according to LEAKE's (1978) classification (*Fig. 3*). The amount of $(Fe^{+2}/Fe^{+2}+Mg)$ ranges from 0.513 to 0.608 mol% (Table 4).

ALTERATION PATTERNS IN THE MINE AREA

a) Alteration minerals

Chlorite is abundantly distributed in the altered zones of the Umm Rus gold mine area. It is mostly formed by replacement of biotite and sometimes hornblende and in relatively strong altered zones the chlorite occurs as a pseudomorphic mineral and may contain relicts of biotite and hornblende (Plate I, A). The chemical data of the analyzed chlorite (Table 5) proved the dominancy of brunsvigite in the studied altered granodiorite (Fig. 4). The use of chlorite as a geothermometer has been discussed by many authors as CATHELINEAU and NIEVA (1985) and CATHELINEAU et al. (1988). They concluded that the Al-content in the tetrahedral site of chlorite is a function of temperature of formation. Using the average mol% of Al in the tetrahedral site and appling their geothermometry, it can be concluded that the present chlorite indicates temperature of formation ranging from 180° to 285°C (*Fig. 5*) with an average 225°C.

In the slightly altered samples, epidote is a common alteration mineral and is closely associated with chlorite (Plate I, A). The current epidote is analyzed (Table 6) and the following ideal formula is deduced: $Ca_{1.991}\ Fe^{+3}_{1.052}\ Al_{1.793}\ (O, OH, SiO_4, Si_{2.098}O_7)$.

Sericite is a common alteration mineral in the study area; it is mostly formed by the alteration of feldspars (Plate I, B). The sericite-content increases towards the quartz vein. The chemistry of sericite (Table 7) reflects that its K-content is distinctly low and

TABLE 1

Selected microprobe analysis of plagioclase feldspars in the Umm Rus granodiorite*

Sample	Albite							Oligoclase				
No.	P1-1	P1-2	P1-3	P1-4	P1-5	P1-6	P1-7	P1-8	P1-9	P1-10	P1-11	P1-12
Na_2O	11.41	11.27	9.80	10.93	11.31	10.87	10.28	9.93	8.44	8.67	8.57	9.10
K_2O	b.d.	b.d.	0.46	b.d.	b.d.	b.d.	b.d.	b.d.	0.28	0.47	0.42	b.d.
CaO	b.d.	b.d.	0.82	b.d.	b.d.	b.d	0.72	2.61	5.19	4.73	4.42	4.49
FeO	b.d.	b.d.	0.12	b.d.	b.d.	b.d.	0.42	b.d.	b.d.	0.23	0.20	b.d.
Al_2O_3	19.93	19.87	20.10	19.50	19.84	19.57	19.69	21.32	23.76	22.55	23.01	22.07
MgO	b.d.	b.d	b.d.	b.d.	b.d.	b.d	b.d.	b.d.	b.d.	b.d.	b.d.	b.d.
SiO_2	68.78	69.21	69.36	69.60	69.29	69.30	68.78	66.35	62.14	63.60	63.01	64.15
Total	*100.12*	*100.35*	*100.66*	*100.03*	*100.44*	*99.74*	*99.89*	*100.21*	*99.81*	*100.25*	*99.63*	*99.81*
Na	0.960	0.944	0.816	0.916	0.947	0.913	0.864	0.842	0.726	0.744	0.737	0.783
K	–	–	0.025	–	–	–	–	–	0.016	0.027	0.024	–
Ca	–	–	0.038	–	–	–	0.033	0.123	0.247	0.224	0.21	0.213
Total	*0.960*	*0.944*	*0.879*	*0.916*	*0.947*	*0.913*	*0.897*	*0.965*	*0.989*	*0.995*	*0.971*	*0.996*
Fe^{+2}	–	–	0.004	–	–	–	0.014	–	–	0.008	0.0007	–
Al	1.018	1.011	1.017	0.993	1.009	0.999	1.006	1.099	1.243	1.177	1.202	1.154
Mg	–	–	–	–	–	–	–	–	–	–	–	–
Si	2.982	2.989	2.979	3.007	2.99	3.001	2.98	2.901	2.7	2.815	2.792	2.846
Total	*4.000*	*4.000*	*4.000*	*4.000*	*4.000*	*4.000*	*4.000*	*4.000*	*4.000*	*4.000*	*4.000*	*4.000*
Ab%	100.00	100.00	92.84	100.00	100.00	100.00	96.32	87.25	73.41	74.77	75.90	78.61
An%	–	–	4.32	–	–	–	3.68	12.75	24.97	22.51	21.63	21.39
Or%	–	–	2.84	–	–	–	–	–	1.62	2.72	2.47	–

* The structural formula of feldspars based on 4 numbers of cations excluding K, Na and Ca
b.d. = below detection

TABLE 2

Selected microprobe analyses of potash-feldspars in the Umm Rus granodiorite*

Sample No.	K-1	K-2	K-3	K-4
K_2O	13.52	15.85	16.71	15.97
Na_2O	0.26	0.34	0.25	0.29
CaO	b.d.	b.d.	0.59	0.66
FeO	0.39	b.d.	0.33	b.d.
Al_2O_3	18.33	19.16	18.69	18.26
SiO_2	67.31	64.64	64.55	65.01
Total	*99.81*	*99.99*	*101.12*	*100.19*
K	0.774	0.927	0.982	0.943
Na	0.023	0.030	0.022	0.026
Ca	–	–	0.029	0.033
Total	*0.797*	*0.957*	*1.033*	*1.002*
Fe^{+2}	0.013	–	0.011	–
Al	0.969	1.036	1.015	0.991
Si	3.018	2.964	2.974	3.009
Total	*4.000*	*4.000*	*4.000*	*4.000*
Or%	97.11	96.87	95.06	94.11
Ab%	2.89	3.13	2.13	2.60
An%	0.00	0.00	2.81	3.29

* The structural formula of feldspars based on 4 numbers of cations excluding K, Na and Ca
b. d. = below detection

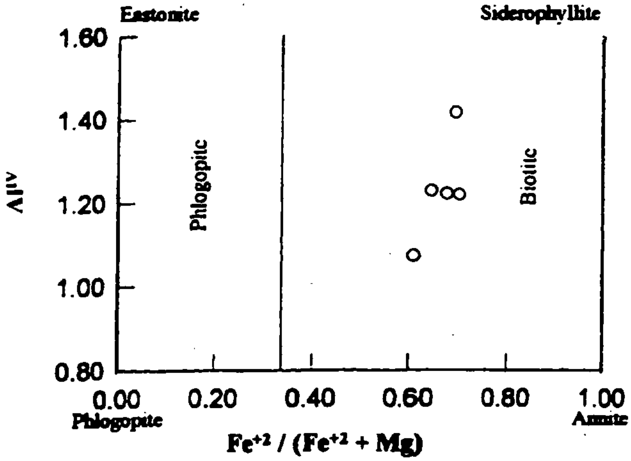

Fig. 2. Classification of biotite from the Umm Rus granodiorite (after DEER et al. 1985)

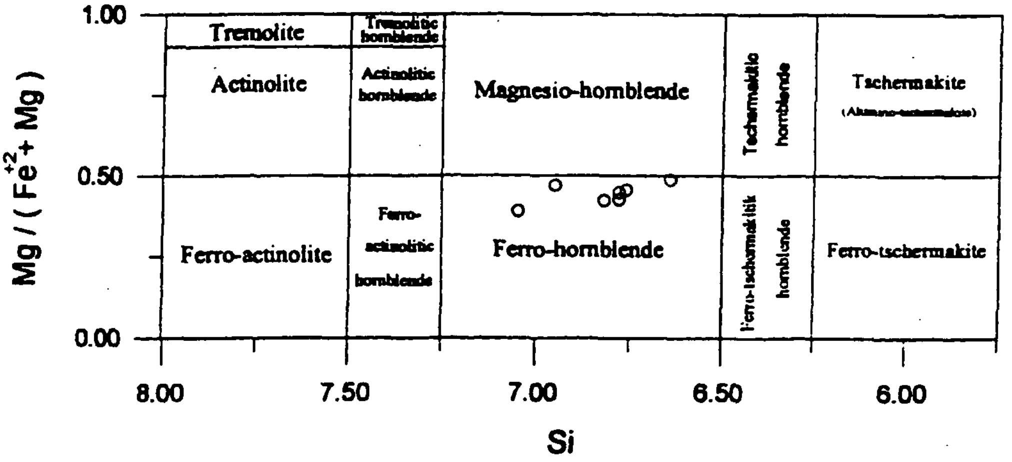

Fig. 3. Classification of amphiboles from the studied granodiorite, in which (Ca+Na)B ≥ 1.34 & NaB < 0.07 (after LEAKE 1978)

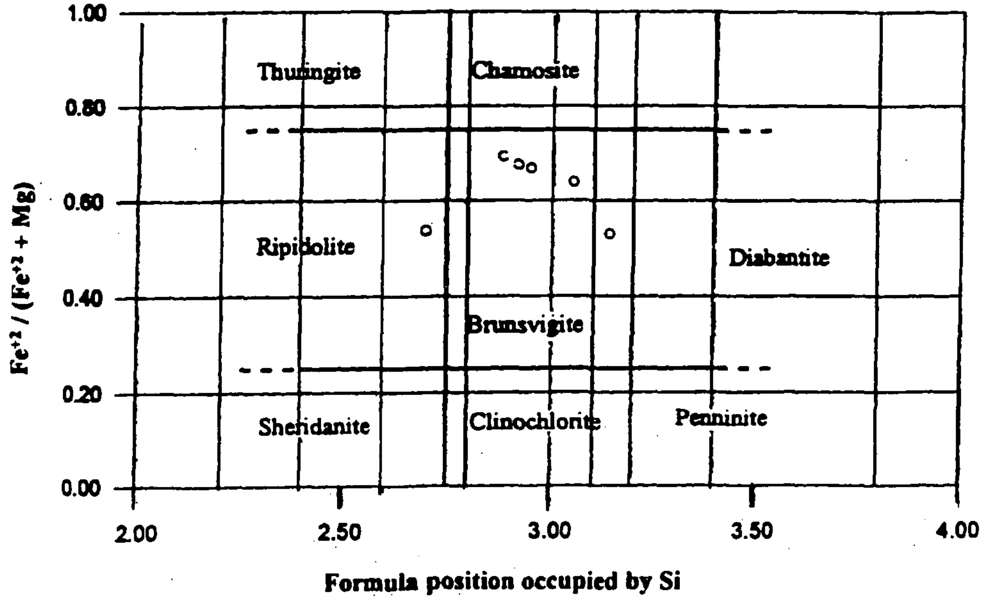

Fig. 4. Chemical classificaton of chlorite, altered from biotite, Umm Rus alteration zones (after FOSTER 1962)

TABLE 3

Selected microprobe analyses of biotite in the Umm Rus granodiorite*

Sample No.	B-1	B-2	B-3	B-4	B-5	B-6
FeO	22.11	23.19	26.05	27.60	27.71	25.42
Fe_2O_3	b.d.	b.d.	b.d.	2.19	b.d.	2.08
MnO	0.12	0.13	0.26	0.30	0.24	0.39
MgO	9.51	8.37	8.19	6.63	7.51	7.93
K_2O	9.03	8.95	7.85	7.07	7.54	7.74
Na_2O	b.d.	b.d.	b.d.	b.d.	b.d.	b.d.
CaO	0.25	0.17	b.d.	b.d.	0.11	b.d.
Al_2O_3	14.14	14.02	15.41	14.60	14.45	15.48
TiO_2	3.87	3.62	3.95	2.07	3.12	1.17
SiO_2	37.09	36.84	36.15	35.36	35.51	35.46
H_2O	3.83	3.77	3.91	3.81	3.83	3.83
Total	*100.22*	*99.06*	*101.77*	*99.63*	*100.02*	*99.50*
K	0.902	0.907	0.772	0.727	0.753	0.772
Na	–	–	–	–	–	–
Ca	0.021	0.014	–	–	0.009	–
H_2O	0.077	0.079	0.222	0.273	0.238	0.228
Total	*1.000*	*1.000*	*1.000*	*1.000*	*1.000*	*1.000*
Fe^{+2}	1.447	1.542	1.691	1.816	1.814	1.662
Fe^{+3}	–	–	–	0.130	–	0.122
Mg	1.109	0.992	0.947	0.777	0.876	0.924
Al	0.208	0.241	0.215	0.135	0.112	0.198
Ti	0.228	0.216	0.130	0.122	0.183	0.068
Mn	0.008	0.009	0.017	0.020	0.016	0.026
Total	*3.000*	*3.000*	*3.000*	*3.000*	*3.000*	*3.000*
Al	1.097	1.072	1.195	1.219	1.221	1.228
Si	2.903	2.928	2.805	2.781	2.778	2.772
Total	*4.000*	*4.000*	*4.000*	*4.000*	*4.000*	*4.000*
OH	1.489	1.464	1.997	1.870	1.972	1.878
O	0.511	0.536	0.003	0.130	0.028	0.122
Total	*2.000*	*2.000*	*2.000*	*2.000*	*2.000*	*2.000*
O	10.000	10.000	10.000	10.000	10.000	10.000
$Fe^{+2}/(Fe^{+2}+Mg)$	0.566	0.609	0.641	0.700	0.674	0.643

* the structural formula of biotite and amphiboles based on 7 and 13 number of cations respectively, excluding K, Na and Ca

b. d. = below detection

TABLE 4

Selected microprobe analyses of amphiboles in the Umm Rus granodiorite*

Sample No.	Am-1	Am-2	Am-3	Am-4	Am-5	Am-6	Am-7
CaO	10.40	10.79	10.63	10.60	10.23	11.23	11.90
Na_2O	1.38	1.54	1.59	1.43	1.48	1.01	0.90
K_2O	0.58	0.71	0.63	0.68	0.66	b.d.	b.d.
FeO	16.49	15.53	17.02	17.52	15.82	16.83	19.72
Fe_2O_3	5.66	8.53	7.27	7.55	8.85	9.01	5.36
MgO	8.25	8.26	7.79	7.24	7.47	6.95	7.12
MnO	0.61	0.66	0.78	0.81	0.93	0.52	0.41
TiO_2	1.51	1.59	1.54	1.57	1.50	b.d.	b.d.
Al_2O_3	6.53	6.90	6.49	6.53	6.70	7.61	6.46
SiO_2	45.62	43.46	44.49	44.38	44.29	44.85	46.29
H_2O	1.97	1.97	1.97	1.96	1.96	1.97	1.97
Total	*99.00*	*99.94*	*100.20*	*100.27*	*99.89*	*99.98*	*100.13*
Na	0.106	0.224	0.209	0.161	0.107	0.131	0.205
K	0.114	0.139	0.123	0.133	0.132	–	–
Total	*0.220*	*0.363*	*0.332*	*0.294*	*0.239*	*0.131*	*0.205*
Na	0.302	0.233	0.262	0.264	0.326	0.168	0.060
Ca	1.698	1.767	1.738	1.736	1.674	1.832	1.940
Total	2.000	2.000	2.000	2.000	2.000	2.000	2.000
Fe^{+2}	2.102	1.985	2.170	2.239	2.021	2.141	2.509
Fe^{+3}	0.649	0.866	0.784	0.827	0.985	1.031	0.613
Mg	1.872	1.881	1.770	1.648	1.703	1.576	1.618
Mn	0.079	0.085	0.100	0.105	0.122	0.066	0.057
Ti	0.173	0.183	0.176	0.181	0.169	–	–
Al	0.125	–	–	–	–	0.186	0.203
Total	*5.000*	*5.000*	*5.000*	*5.000*	*5.000*	*5.000*	*5.000*
Al	1.047	1.242	1.166	1.177	1.205	1.179	0.951
Si	6.953	6.642	6.784	6.781	6.763	6.821	7.049
Fe^{+3}	–	0.116	0.050	0.042	0.032	–	–
Total	*8.000*	*8.000*	*8.000*	*8.000*	*8.000*	*8.000*	*8.000*
OH	2.000	2.000	2.000	2.000	2.000	2.000	2.000
O	22.000	22.000	22.000	22.000	22.000	22.000	22.000
$Mg/Fe^{+2}+Mg$	0.471	0.487	0.449	0.424	0.457	0.424	0.392
$Fe^{+2}/Fe^{+2}+Mg$	0.529	0.513	0.551	0.576	0.543	0.576	0.608

TABLE 5

Selected microprobe analyses of chlorite in the Umm Rus alteration zones*

Sample No.	Ch-1	Ch-2	Ch-3	Ch-4	Ch-5	Ch-6
Fe_2O_3	b.d.	b.d.	1.00	b.d.	0.52	b.d.
FeO	25.03	27.78	32.85	34.19	34.76	28.51
MnO	b.d.	b.d.	0.52	0.54	0.51	0.23
MgO	12.46	8.8	9.4	8.45	9.47	13.79
CaO	0.24	0.19	n.d.	0.54	0.11	0.21
K_2O	0.14	0.34	1.13	0.32	0.62	b.d.
Na_2O	b.d.	0.11	b.d.	b.d.	b.d.	b.d.
Al_2O_3	21.44	23.5	16.35	17.86	17.02	19.79
TiO_2	b.d.	b.d.	0.27	1.81	0.21	1.07
SiO_2	29.82	28.46	26.58	26.32	26.8	25.52
H_2O	11.38	11.19	10.82	10.95	11.02	11.32
Total	*100.51*	*100.37*	*98.92*	*100.98*	*101.04*	*100.32*
Mg	1.203	0.985	1.552	1.379	1.536	1.723
Fe^{+3}	–	–	0.088	–	0.042	–
Fe^{+2}	–	–	0.208	0.238	0.26	–
Al	1.797	2.015	1.081	1.184	1.098	1.172
Mn	–	–	0.048	0.05	0.047	0.02
Ti	–	–	0.023	0.149	0.017	0.085
Total	*3.000*	*3.000*	*3.000*	*3.000*	*3.000*	*3.000*
Si	3.138	3.048	2.945	2.881	2.915	2.702
Al	0.862	0.952	1.055	1.119	1.085	1.298
Total	*4.000*	*4.000*	*4.000*	*4.000*	*4.000*	*4.000*
Mg	0.751	0.42	–	–	–	0.453
Fe^{+2}	2.203	2.489	2.841	2.892	2.902	2.524
Ca	0.027	0.021	–	0.063	0.012	0.023
K	0.019	0.047	0.159	0.045	0.086	–
Na	–	0.023	–	–	–	–
Total	*3.000*	*3.000*	*3.000*	*3.000*	*3.000*	*3.000*
OH	8.000	8.000	8.000	8.000	8.000	8.000
O	10.000	10.000	10.000	10.000	10.000	10.000
$Fe^{2+}/(Fe^{+2}+Mg)$	0.530	0.639	0.663	0.694	0.693	0.539

TABLE 6

Selected microprobe analyses of epidote in the Umm Rus alteration zones*

Sample No.	Ep-1	Ep-2	Ep-3
Fe_2O_3	17.10	16.78	17.30
MgO	0.24	0.23	0.23
CaO	22.75	22.99	22.25
SrO	0.20	0.10	0.13
Al_2O_3	18.51	18.97	18.21
TiO_2	0.53	0.41	0.49
SiO_2	37.83	37.53	38.01
H_2O	3.44	3.66	3.34
Total	*100.60*	*100.67*	*99.96*
Ca	1.995	2.014	1.964
Sr	0.010	0.005	0.006
Mg	0.029	0.028	0.028
Total	*2.034*	*2.047*	*1.998*
Al	1.784	1.828	1.768
Ti	0.034	0.025	0.030
Fe^{+3}	1.052	1.032	1.073
Total	*2.870*	*2.885*	*2.871*
Si	3.096	3.068	3.131
Al	–	–	–
Total	*3.096*	*3.068*	*3.131*
$Fe^{+2}/(Fe^{+2}+Al)$	0.371	0.361	0.378

* the structural formula of chlorite and epidote based on 10 and 8 number of cations respectively

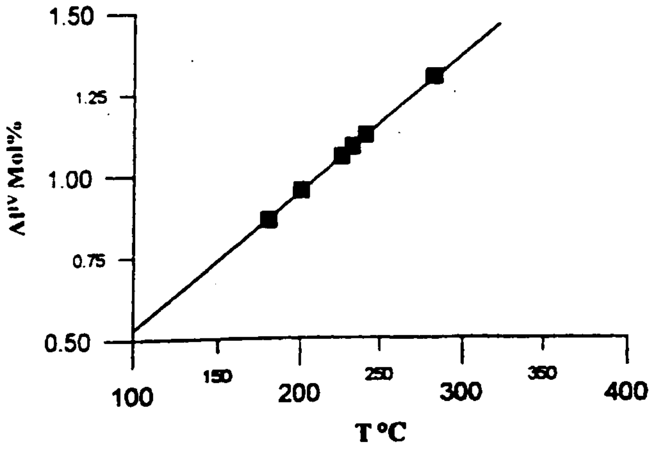

Fig. 5. Plot of Al^{IV} versus temperature for the chlorite available in the Umm Rus alteration zones (after CATHELINEA et al. 1988)

consequently the H_2O in the K-position is high. Accordingly, the sericite from the studied area can be classified as hydrosericite.

Two *carbonate* generations are distinguished in the altered zones of the Umm Rus granodiorite; less abundant calcite (generation I) and relatively abundant ankerite (generation II). Calcite occurs mostly as very fine-grained aggregates essentially replacing plagioclase, chlorite and hornblende. The chemical data presented in Table 8 show that the $CaCO_3$-content in calcite ranges from 94.42 to 98.60 mol%; the $MgCO_3$-component ranges from 1.40 to 2.03 mol%, while siderite and rhodochrosite are of minor significance. Ankerite is frequently present in altered sulphide-rich samples. It seems to replace chlorite (Plate I, C), plagioclase and sericite. The mineral chemistry reflects an ex-solution of dolomite-ankerite. The dolomite ranges from 36.52 to 59.84 mol%; and ankerite has a range of 35.42 to 62.60 mol% (Table 8). Thus the chemical formula of the minerals ranges from dolomitic-ankerite $[Ca_{.973}\ Mg_{.365}\ (Fe_{.648}Mn_{.014})_{.662}]_2\ (CO_3)_2$ to ankeritic-dolomite $[Ca_{.953}\ Mg_{.598}\ (Fe_{.426}\ Mn_{.023})_{.449}]_2\ (CO_3)_2$. A siderite component is also recorded on the ankerite as a solid solution up to 4.74 mol%.

Sulphidization is a common process in the Umm Rus gold mine. Most sulphides occur in the alteration zones and subordinately in the quartz vein. Pyrite, arsenopyrite and pyrrhotite are the common sulphide phases. Gold appears as specks in pyrite and aresenopyrite and sometimes it is filling fractures of the brecciated pyrite. *Silicification* is the most intensive alteration process due to hydrothermal acitivity in the study gold mine area. The dominant quartz veins have been most probably produced during this relatively young alteration process.

b) Alteration zones

The various alteration mineral assemblages characterizing distinct alteration zones (*Fig. 6*) in the granodiorite of the Umm Rus area can be divided into the following:

1. Chlorite-epidote zone (Zone R1)

This alteration zone is occured far away from the quartz vein (*Fig. 6*). This mineral assemblage is characterized by the predominance of chlorite and epidote formed as a result of biotite alteration (Plate I, A). Hornblende and K-feldspar in this zone are usually unaltered, whilst plagioclases are slightly sericitized.

2. Sericite-chlorite zone (Zone R2)

In this zone, many of the primary minerals are almost altered. Sericite and subordinate chlorite are the main alteration products. Calcite is the only distinguished carbonate, it is uncommon alteration product. Silicification is also present in this alteration zone, where silica occurs as a replacement mineral, filling cavities and/or formating quartz veinlets.

3. Sericite-ankerite-chlorite-sulphides zone (Zone R3)

This alteration zone is observed close to and in contact of the central quartz vein (Fig. 6). Minerals characterizing this zone are sericite, ankerite, chlorite and sulphides. Ankeritic carbonatization and sulphidization are the diagnostic feature in this zone. Ankerite seems to replace mainly chlorite (Plate I, C) and sometimes sericite. Most sulphide crystals as pyrite and arsenopyrite contain relics of wall rock material revealing a strong sulphidization of the pre-existing minerals.

4. Quartz-carbonates-sulphides-wall rock relicts zone (Zone R4)

SiO_2-rich fluids resulted in silicification of the previously formed minerals and deposition of the quartz vein. Many relicts of carbonates, wall rock material and sericite (Plate I, D) are recorded in this alteration zone. Some of these are arranged parallel to the foliation of the wall rocks (Plate I, E). On the other hand, sulphides prevailed in this zone are more resistant against silicification than the other minerals and thus generally exhibit a relatively less degree of silicification (Plate I, F).

c) Geochemistry

Ion exchange between wall rock and ore-bearing fluids is the principal chemical process operative during the hydrothermal alteration. One approach to examine the chemical aspects of alterations is to determine the gain and loss of components in the entire rock mass during metasomatism and to refer these alterations to the observed mineral assemblages. The whole rock chemical composition of the Umm Rus gold mine lithologes of the different alteration zones and the unaltered granodiorite are presented in Table 9.

Mass balance calculations

The principles of mass balance are compatible to those described by MACLEAN and KRANIDIOTIS (1987). This method depends on the nature of the precursor rock. At the Umm Rus gold mine area, the fresh granodiorite is the only precursor which seems to be more or less chemically homogeneous (single precursor system). According to MACLEAN and KRANIDIOTIS (op. cit.) method, it is found that the most immobile element pair is Al_2O_3-Zr. The selection of such elements is based on: their proper linear regression relation, the high correlation coefficient and passing of the line relation through both the point of origin and the average bulk composition of the fresh granodiorite (*Fig. 7*). Al_2O_3 is preferred to be a monitor for the mass change calculation rather than Zr for its better correlation with the other elements. TiO_2 followed by Ba, Rb and Ga are relatively slight mobile. The gain and loss of chemical components were calculated by assuming a starting mass of 100 g of the fresh granodiorite according to the following formula:

Component "A"g = component A / Al_2O_3 wt% in altered rock x Al_2O_3 in fresh rock.

The results of mass gain and loss of the different alteration zones are given in Table 10 and illustrated in *Fig. 14*. The following is a brief discussion of the mass changes for each alteration zone:

1. Chlorite-epidote zone (R1)

The main chemical changes in this zone have involved the addition of SiO_2, Fe_2O_3, Na_2O and volatiles (L.O.I.), while losses took place in K_2O, CaO, and MgO (*Fig. 8a*). The gain of SiO_2 means that the silica added by silicification was more than that lost by the alteration of biotite to chlorite and epidote. The addition of iron and volatiles resulted in the formation of new iron-bearing hydrous phases, principally chlorite. The small loss of K indicates that the amount of sericite formed in this zone is not enough to consume all the K released from biotite during its alteration to chlorite and epidote. Thus, most of the remaining K was carried away in solution. The partial alteration of plagioclase to sericite led to the release of Ca which was partially used in the formation of epidote while the rest was lost from the system. The depletion in Mg in this zone may also be attributed to the chloritization of biotite. The main chemical changes among the trace elements is the gain of Sr. The mineral analysis indicate that epidote is the main Sr-bearing phase in this alteration zone.

2. Sericite-chlorite zone (R2)

Chemical changes in this zone seem to be mainly a result of two alteration processes: sericitization and chloritization. Sericitization of plagioclase feldspars yields a strong

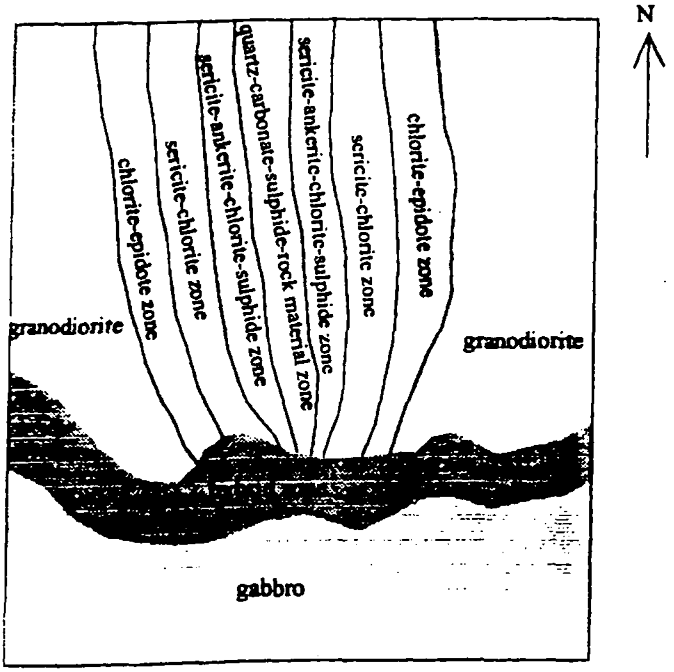

Fig. 6. Sketch illustrating the distribution of alteration zones and quartz vein in the Umm Rus gold mine

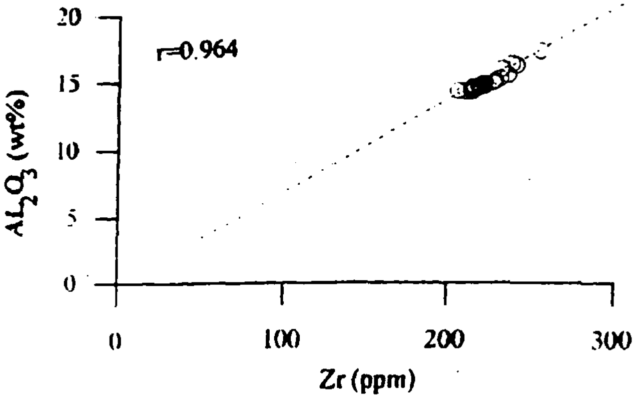

Fig. 7. Variation diagram illustrating the most two immobile elements (r = correlation coefficient).

● = average composition of fresh granodiorite ○ = altered samples

TABLE 7

Selected microprobe analyses of sericite in the Umm Rus alteration zones*

Sample No.	Sr-1	Sr-2	Sr-3	Sr-4	Sr-5	Sr-6	Sr-7
K_2O	6.33	6.71	4.89	9.25	5.63	6.28	5.25
Na_2O	0.33	0.15	0.11	0.19	0.16	0.29	0.27
CaO	b.d.	b.d.	0.53	0.48	b.d.	b.d.	b.d.
FeO	1.05	1.85	2.28	1.16	3.54	1.15	2.04
MgO	0.60	1.17	0.65	0.43	1.77	0.48	0.93
Al_2O_3	36.84	34.68	35.76	35.40	30.15	36.29	33.43
TiO_2	b.d.	0.30	b.d.	0.56	0.21	0.19	0.16
SiO_2	50.46	50.01	49.66	49.50	54.14	50.21	53.42
H_2O	4.77	4.72	4.73	4.64	4.75	4.74	4.79
Total	*100.38*	*99.59*	*98.61*	*101.32*	*100.36*	*99.63*	*100.29*
K	0.543	0.587	0.395	0.762	0.517	0.566	0.467
Na	0.043	0.020	0.013	0.024	0.022	0.040	0.037
Ca	–	–	0.036	0.033	–	–	–
(H_2O)	0.414	0.393	0.556	0.181	0.461	0.394	0.496
Total	*1.000*	*1.000*	*1.000*	*1.000*	*1.000*	*1.000*	*1.000*
Fe^{+2}	0.055	0.098	0.121	0.063	0.186	0.061	0.107
Mg	0.056	0.111	0.061	0.041	0.166	0.045	0.086
Al	1.889	1.777	1.818	1.869	1.637	1.885	1.799
Ti	–	0.014	–	0.027	0.010	0.009	0.008
Total	*2.000*	*2.000*	*2.000*	*2.000*	*2.000*	*2.000*	*2.000*
Al	0.835	0.821	0.853	0.803	0.597	0.822	0.663
Si	3.165	3.179	3.147	3.197	3.403	3.178	3.337
Total	*4.000*	*4.000*	*4.000*	*4.000*	*4.000*	*4.000*	*4.000*
OH	2.000	2.000	2.000	2.000	2.000	2.000	2.000
O	10.000	10.000	10.000	10.000	10.000	10.000	10.000
(H_2O)	2.000	2.000	2.000	2.000	2.000	2.000	2.000

* the structural formula of sericite based on 6 number of cations excluding K, Na and Ca
b.d. = below detection

TABLE 8

Selected microprobe analyses of carbonate generations in the Umm Rus alteration zones*

Sample	generation I			generation II								
No.	Car-1	Car-2	Car-3	Car-4	Car-5	Car-6	Car-7	Car-8	Car-9	Car-10	Car-11	Car-12
MgO	0.56	0.82	0.57	8.76	12.31	7.19	7.96	9.36	7.32	8.48	8.54	8.4
CaO	55.28	53.02	55.24	26.75	27.26	26.62	27.72	27.55	27.59	27.57	27.56	27.51
FeO	b.d.	2.05	b.d.	20.46	16.62	22.72	20.19	18.46	21.34	19.48	19.62	19.83
MnO	b.d.	0.5	b.d.	0.68	0.83	0.5	0.81	0.92	0.72	0.97	0.72	0.77
SrO	b.d.	b.d.	b.d.	b.d.	b.d.	b.d.	b.d.	b.d.	b.d.	b.d.	0.11	b.d.
CO_2	44.01	43.17	43.98	43.51	44.91	42.96	43.3	43.72	43.15	43.43	43.47	43.39
Total	*99.85*	*99.56*	*99.79*	*100.2*	*100.9*	*99.99*	*99.98*	*100*	*100.1*	*99.93*	*100*	*99.90*
Calcite	98.60	94.42	98.59	–	–	–	0.50	–	0.40	–	–	–
Magnesite	1.40	2.03	1.51	–	–	–	–	–	–	–	–	–
Dolomite	–	–	–	43.96	59.84	36.52	40.10	46.76	37.00	42.60	42.90	42.30
Siderite	–	2.85	–	3.50	4.74	2.74	–	1.10	–	0.30	0.40	0.50
Ankerite	–	–	–	52.54	35.42	60.74	59.40	52.14	62.60	57.10	56.60	57.20
Strontiarite	–	–	–	–	–	–	–	–	–	–	0.10	–
Rhodochrosite	–	0.70	–	–	–	–	–	–	–	–	–	–

The structural formulae of carbonates were calculated on the basis of 1 cation for minerals having calcite-structure and 2 cations for those having dolomite-structure CO_2 was added by calculation.
b.d. = below detection

depletion in Ca and Na, while chloritization of biotite produces high K concentration in the rock. Some of the released K was probably used during the potassic alteration of the plagioclase feldspars. These two hydrothermal processes may also lead to a loss in SiO_2 due to the expected leaching of silica, and gain in H_2O. The main chemical changes among the trace elements are a depletion in Sr and Zn, and a gain of Ba, Rb and Ni (Table 10 and *Fig. 8b*).

3. Sericite-ankerite-chlorite-sulphides zone (R3)

The average chemical compositon of this zone shows that there is a relatively strong depletion in Si and Na. The volatile constituents, K, Fe and little amounts of Ca and Mg were added to the system. The main chemical changes among the trace elements involved losses in Sr and Zn and gains in Rb and Ba. Slight gains in Ga, Ni and V are also recorded. The loss of SiO_2 from this zone could suggest either:

a) removal of silica during the breakdown of original silicate minerals. Microscopically, all the primary silicate minerals, except quartz, were altered, or
b) leaching of quartz. BÖHLKE (1989) showed that primary quartz was leached from the granodioritic wall rock during mineralization processes.

The loss of Na might have been resulted from the breakdown of plagioclase feldspars to sericite. The slight enrichment of Ca in this zone advocates that the Ca released from the breakdown of amphiboles and plagioclase feldspars was held up in the newly formed ankerite. The enrichment in K and volatiles in this zone reflects the intensity of sericitization. As ankerite is abundant in this zone, the expected composition of the volatile constituents should be mainly water and CO_2.

Most sulphide minerals in the Umm Rus gold mine area are found in this zone. Microscopically, sulphides are intergrown with and replace iron-bearing silicate and oxide

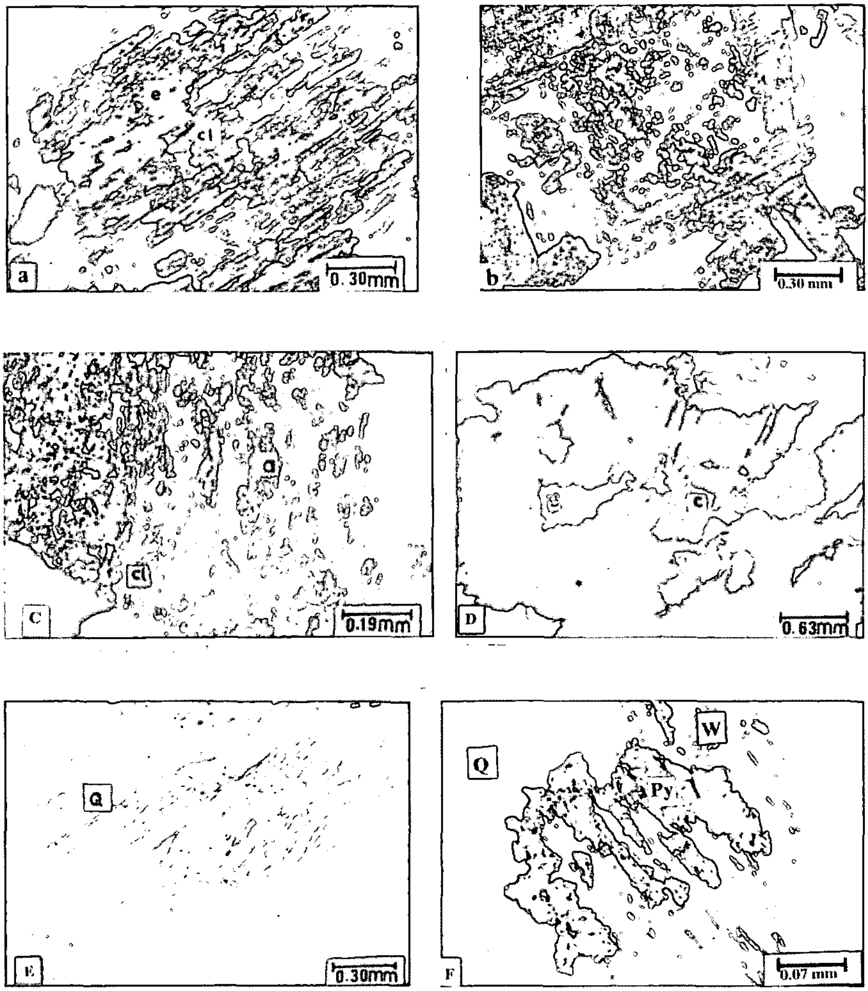

Plate I

A: Pseudomorphic chlorite (cl)-epidote (e) after biotite. Chlorite-epidote zone, R1 (C. N.)

B: Incomplete sericitization of coarse-grained plagioclase feldspar crystal (at the middle). Sericite-chlorite zone, R2 (C. N.)

C: Chlorite (cl) partially replaced by ankerite (a) "carbonate generation II.". Sericite-ankerite-chlorite-sulphide zone, R3 (C. N.)

D: Relics of fine-grained calcite (c) and sericite aggregates (s) are placed in coarse grained quartz. Quartz vein, R4 (C. N.)

E: Inclusions of mixed carbonate and sericite in coarse-grained quartz, note that these inclusions are arranged parallel to each other and to the foliation of the wall rock. Quartz vein, R4 (C. N.)

F: Replacement of pyrite (py) and wall rock material (w) by silica. Irregular contact between pyrite crystal and quartz is noticed. Quartz vein R4 (C. N.)

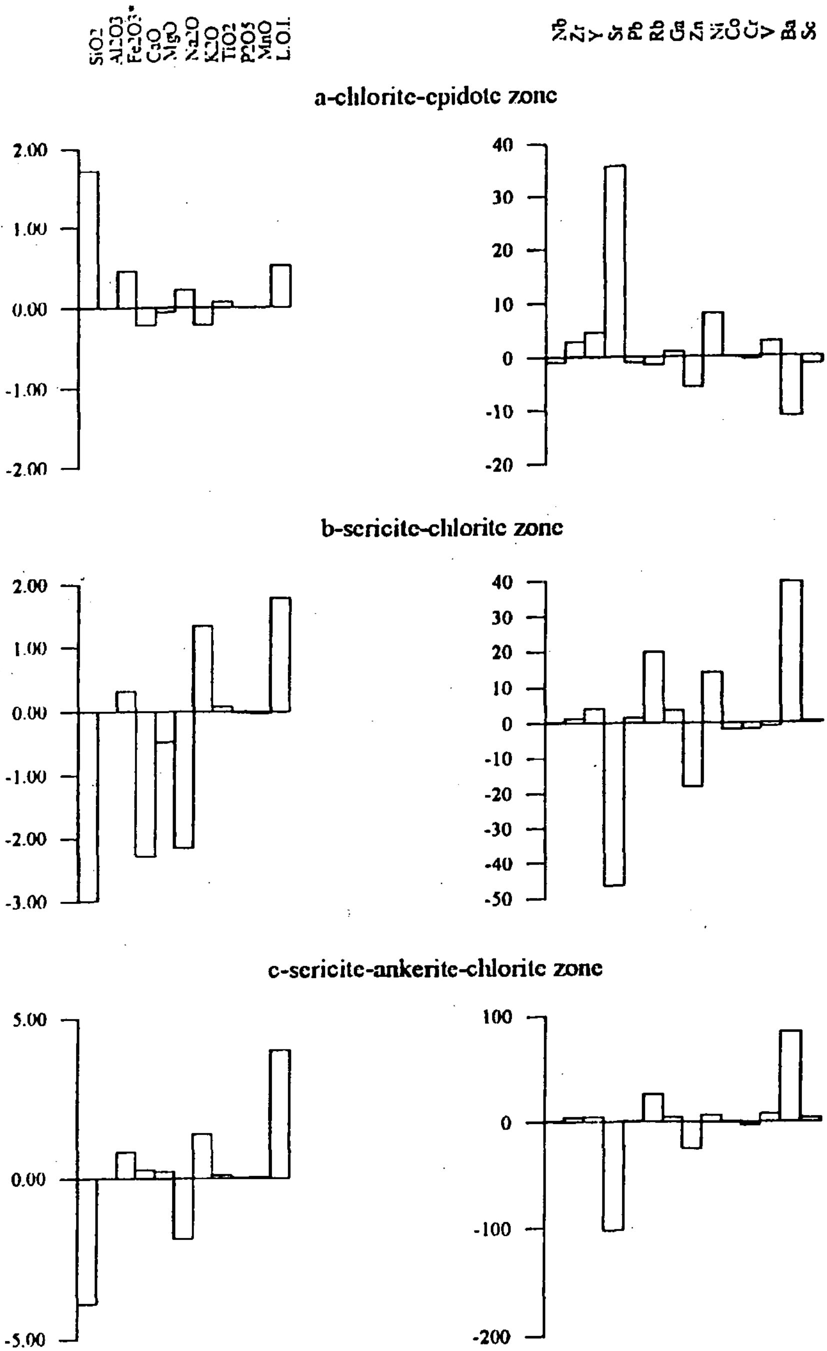
a-chlorite-epidote zone

b-sericite-chlorite zone

c-sericite-ankerite-chlorite zone

Fig. 8. Gains and losses in the alteration zones of the Umm Rus gold mine area. (major elements in wt%, trace elements in ppm).

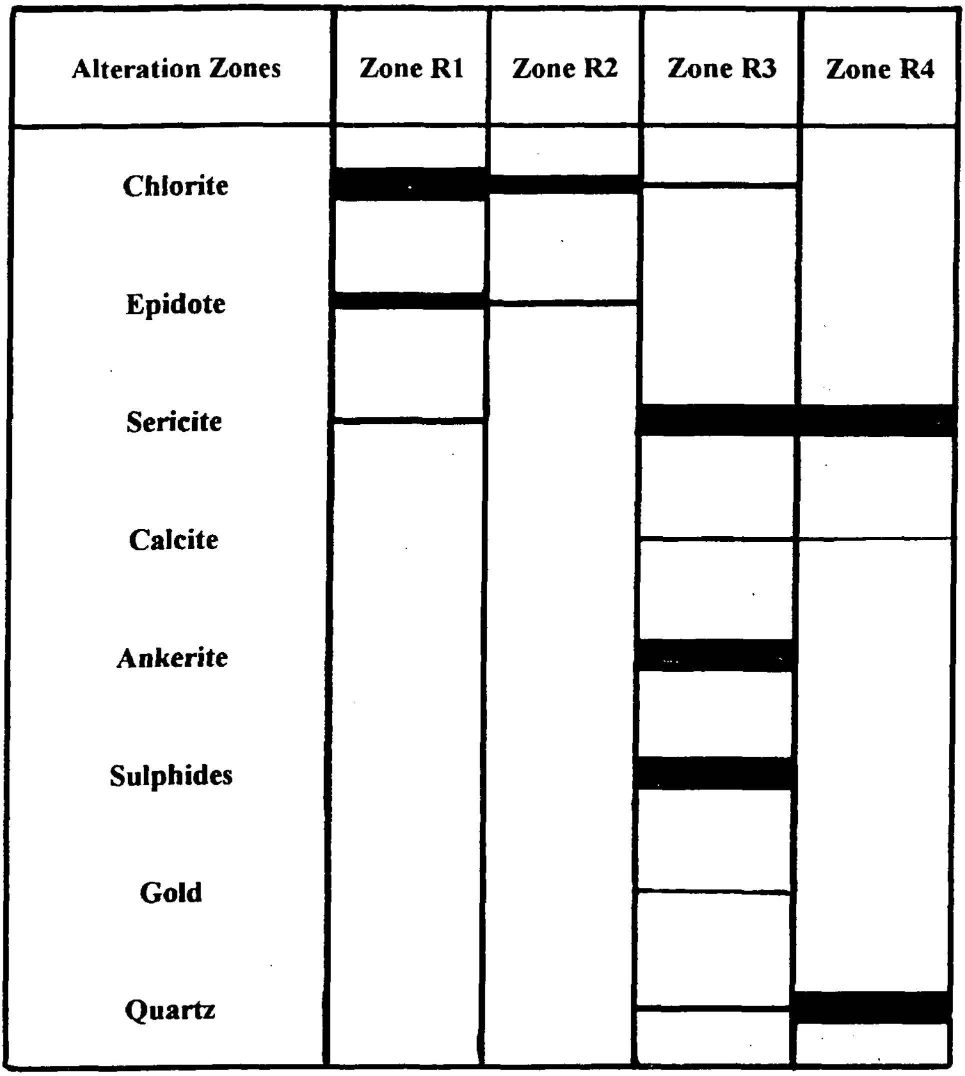

Fig. 9. Paragenetic sequence of the alteration minerals in the Umm Rus gold mine.
(Thickness of lines indicates the mineral abundance)

TABLE 9

Chemical composition of fresh granodiorite and its alteration zones in the Umm Rus gold mine area

Oxides	Fresh granodiorite		Chlorite-epidote		Sreicite-chlorite zone		Sericite-ankerite-chlorite-sulphides zone		Quartz vein	
wt%	Range	Mean(n=5)	Range	Mean(n=6)	Range	Mean(n=7)	Range	Mean(n=6)	Range	Mean(n=3)
SiO_2	67.20–68.40	67.6	66.40–67.90	67.47	65.30–70.90	67.49	61.50–63.80	62.85	> 99.5	> 99.50
Al_2O_3	14.60–15.80	15.02	14.30–15.00	14.62	14.40–17.40	15.69	14.30–15.30	14.83	< 0.1	< 0.10
Fe_2O_3	1.04–1.45	1.17	1.01–1.57	1.25	1.50–3.91	2.88	1.50–3.85	2.50	0.25–0.36	0.30
FeO	2.53–3.33	3.02	2.75–3.36	3.09	1.50–3.60	2.00	2.22–2.78	2.50	0.03–0.06	0.05
CaO	3.22–3.48	3.36	2.87–3.28	3.07	0.24–3.09	1.12	3.19–3.87	3.57	0.03–0.08	0.04
MgO	1.06–1.31	1.16	0.99–1.18	1.08	0.29–1.05	0.72	0.94–1.75	1.34	< 0.01	< 0.01
Na_2O	4.39–4.57	4.48	4.41–4.84	4.57	0.89–3.67	2.42	1.48–3.59	2.53	< 0.01	< 0.01
K_2O	2.10–2.26	2.19	1.48–2.07	1.93	2.50–5.03	3.69	2.59–4.54	3.52	< 0.01	< 0.01
TiO_2	0.50–0.55	0.52	0.55–0.57	0.57	0.54–0.70	0.63	0.09–0.40	0.59	0.02–0.04	0.03
P_2O_5	0.13–0.15	0.14	0.13–0.15	0.14	0.06–0.16	0.13	0.55–0.66	0.58	< 0.01	< 0.01
MnO	0.08–0.11	0.09	0.07–0.11	0.09	0.01–0.10	0.06	0.12–0.18	0.14	< 0.01	< 0.01
H_2O	0.12–0.16	0.14	0.11–0.22	0.17	0.21–0.38	0.22	0.09–0.15	0.11	< 0.01	< 0.01
L.O.N.	0.79–1.08	0.932	1.00–2.23	1.41	2.01–4.36	2.84	3.72–6.32	4.88	0.20–0.22	0.21
Total	*99.56–100.14*	*99.822*	*98.72–100.28*	*99.46*	*99.90–100.52*	*99.89*	*99.21–99.48*	*99.94*	*100.10–100.60*	*100.15*
Nb	6–7	6.6	4–8	5.50	6–10	7.14	5–11	7.33	b.d. – 1	0.83
Zr	206.9–244.7	220	210–226	217.00	206–255	231.14	215–230	221.17	9–10	9.67
Y	30–36	33.4	35–39	37.00	31–57	39.14	33–45	37.33	b.d. – 2	1.00
Sr	201–228	213.8	202–318	242.83	57–607	174.86	66–146	110.00	1–15	10.00
Pb	7–13	10.6	7–12	9.33	9–18	12.57	60–98	77.00	1–4	2.67
Rb	50–54	51.8	40–55	49.00	39–118	74.71	9–15	11.00	5–11	2.67
Ga	14–18	16.2	14–21	16.67	16–27	20.57	17–26	20.17	b.d.	b.d.
Zn	53–76	63.2	30–73	56.17	9–75	47.00	28–44	37.67	b.d.	b.d.
Ni	1–14	7.8	n.d. – 54	15.50	n.d. – 37	22.86	4–26	14.17	3–28	12.67
Co	10–11	10.4	8–11	10.00	5–12	8.86	5–13	10.83	2–4	2.67
Cr	12–17	13.6	11–15	12.83	9–16	12.43	7–13	10.83	66–73	69.00
V	44–50	47	49–51	48.50	26–69	48.00	46–60	53.83	4–8	5.67
Ba	450–491	467	358–493	443.67	335–738	529.14	443–708	544.83	b.d. – 17	7.33
Sc	9–13	10.8	6–12	9.17	7–20	11.71	9–22	14.17	b.d. – 1	0.30

Major oxides in wt% and trace elements in ppm
b.d. = below detection. Mean is calculated by excluding the values below detection limit.

TABLE 10

Mass exchange or the altered zones compared to fresh granodiorite in the Umm Rus gold mine area

Oxides and elements	Fresh granodiorite	Chlorite-epidote zone	Sericite-chlorite zone	Sericite-ankerite chlorite zone
SiO_2	67.60	1.72	–2.99	–3.94
Al_2O_3	15.02	0.00	0.00	0.00
Fe_2O_3*	4.53	0.46	0.32	0.82
CaO	3.36	–0.21	–2.29	0.26
MgO	1.16	–0.05	–0.47	0.20
Na_2O	4.48	0.22	–2.16	–1.92
K_2O	2.19	–0.21	1.34	1.38
TiO_2	0.52	0.07	0.08	0.08
P_2O_5	0.14	0.00	–0.02	0.01
MnO	0.09	0.00	–0.03	0.02
L.O.I.	0.93	0.52	1.79	4.01
Nb	6.60	–0.95	0.24	0.82
Zr	220.00	2.94	1.27	4.00
Y	33.40	4.61	4.07	4.41
Sr	213.80	35.67	–46.41	–102.39
Pb	10.60	–1.01	1.43	0.54
Rb	51.80	–1.46	19.72	26.19
Ga	16.20	0.93	3.49	4.23
Zn	63.20	–5.49	–18.21	–25.05
Ni	7.80	8.12	14.08	6.55
Co	10.40	–0.13	–1.92	0.57
Cr	13.60	–0.42	–1.70	–2.63
V	47.00	2.83	–1.05	7.52
Ba	467.00	–11.19	39.54	84.81
Sc	10.80	–1.38	0.41	3.55

* total iron as Fe_2O_3
Major oxides in wt%, trace elements in ppm

minerals. The presence of rutile, pseudorutile and leucoxene relicts which are a common feature in the sulphide grains, especially arsenopyrite and pyrite, supports the mentioned interpretation. It could suggest that sulphur and arsenic which originated from hydrothermal fluids reacted with iron in iron-bearing silicates and oxides (e.g. biotite, chlorite, magnetite and ilmenite) in the host rock to produce pyrite and arsenopyrite in the altered rock. Similar conclusions were reached by SAUNDERS and TUACH (1991) in the study of alteration processes in Rattling Brook Deposits, Canada. Sulphidation of primary Fe-bearing phases is a typical feature characterizes mesothermal gold deposits (COLVINE et al., 1984; GROVES and PHILLIPS, 1987 and BÖHLKE, 1989).

DISCUSSION AND CONCLUSION

In the light of the foregoing discussion, the following arguments can be concluded.

1. In the Umm Rus gold mine area, the main quartz veins cross-cut the granodiorite, the adjacent hybrid zones and gabbros. This indicates that the quartz veins are post-date than the magmatic event, i. e. the gold deposits show no close time relation to the granitic or the basic igneous bodies.
2. The gold mineralization in the studied mine area appears to be structurally controlled. The gold deposit is restricted to shear zones and fractures along which the mineralizing fluids penetrate the pre-existing wall rocks leaving behind different types of alteration zones.
3. The distribution of alteration zones around the main quartz vein has a more or less symmetrical patterns. Through these zones, the amounts of chlorite and epidote decrease whilst sericite, carbonates and sulphides increase towards the central quartz vein.
4. The textural relationship among the alteration minerals indicate that chlorite and epidote were formed firstly, followed by sericite and then by ankerite and sulphides (*Fig. 9*). All the studied mineral phases were affected by silicification.
5. The sulphides-gold specks-carbonates associations occur in both the quartz veins and the altered host rocks represent the last stable phases in the SiO_2-rich solutions. Therefore, they are relatively concentrated along shear zones through which SiO_2-rich solutions coming out causing silicification of the pre-existing rocks and forming the present quartz veins. The following aspects put the previous belief, that the quartz veins and the mineralization were cogenetic, in considerable doubt:

(i) the sulphides in the quartz veins are mostly associated with carbonates and relics from the wall rock materials. The so-called grey quartz appears to be richer in sulphides, carbonate relics and wall rock inclusions than in the milky one.

(ii) the presence of undigested wall rock material and xenoliths in sulphides is a dominant phenomenon.

(iii) the distribution of sulphides appear to be widely variable among gold mines in the Eastern Desert of Egypt, as well as within the same gold mine. In some gold deposits, the sulphides are more concentrated in the quartz veins (e. g. El-Sid mine), in others the sulphides are concentrated in the wall rock alteration zones (e. g. Umm Rus mine). If the sulphides and the quartz veins are cogenetic, such sulphides should be more or less regular in their distribution or even more concentrated in the quartz veins. Additionally, in other gold mines, many quartz veins are barren of any sulphides.

6. The patterns of alteration zones appear to be controlled by the wall rock--hydrothermal fluid interaction. The dominancy of the studied alteration phases indicates that the affecting hydrothermal solutions were enriched in H_2O and CO_2. As the amounts of sericite, ankerite and sulphides increase near the contact with the qurtz vein, this indicates a noticeable addition of K, S, H_2O and CO_2 by the progress of alteration from fresh granodiorite to quartz vein. Some other elements such as As, Zn, Pb, Cu and Au are also added to the system during the alteration events.
7. Most elements (trace and major ones) do not show strong mobilities in most of the alteration zones. Therefore, the mass balance (gains and losses) shows a limited range for element concentrations in these zones.

GENETIC MODEL

The interpretations of the combined geological, mineralogical and geochemical data in the present work aim at formulating a genetic model (*Fig. 9*) for the alteration zones which can be summarized in the following:

a) The hydrothermal fluids, were derived from below through N-S shear zones in the inspected mine area. At the begining of invasion, these fluids were characterized by low CO_2/H_2O ratio which easily altered the pre-existing biotite to some iron-bearing hydrous phases as chlorite and epidote. Some other ferromagnesian minerals e.g. hornblende are noticed to be unaffected by these fluids. The CO_2 content of fluids was not enough to permit the carbonates formation at this early stage of alteration. The geothermometry of the studied chlorite indicates its formation at about 225°C.

b) The fluids of the second stage became enriched in K after the biotite alteration in stage A. These fluids reacted with plagioclases to form sericite. The alteration of plagioclases to K-feldspars was accelerated by the K-enriched fluids. In this stage, the CO_2/H_2O ratio is still low, as indicated from the high H_2O content in the sericite (Table 7).

c) As the chlorite, epidote and sericite were formed, the proportion of H_2O decreased and then the CO_2/H_2O ratio became high in the fluids. Consequently, ankerite was originated in this stage. Sulphides characterizing zone R3 were concomitant with conspicuous concentration of Fe, As, Cu and Au. The presence of these sulphides suggests reducing environmental conditions. It is easily noticed that the given iron by the breakdown of the ferromagnesian minerals was completely consumed in the formation of the iron-bearing sulphide minerals.

d) The last stage is characterized by severe silicification that led to the formation of the quartz veins. All the previous stages were affected by this silicification. The intensity of silica replacement depends on the mineral compositions. Ankerite, chlorite, epidote, and sericite show strong and sometimes complete silicification, on the other hand, sulphides were weakly affected by SiO_2-rich solution. This solution is reworked and dissolved the pre-existing native gold in sulphides and then redistributed the gold in some sulphide phases e.g. pyrite and pyrrhotite. The enrichment of gold by this proposed process is advocated by MÜCKE and ADJIMAH (1994) on gold deposits of Prestea and Obuasi, Ashanti Belt, Ghana. However, the detailed work concerning the gold enrichment of the Umm Rus gold mine will be published elsewhere by the same authors.

ACKNOWLEDGEMENTS

The authors are grateful to Professor A. MÜCKE of Georg-August University, Göttingen, Germany for the facilities offered during the microprobe analysis. They are also indebted to Mr. ELLIS of the same university who helped in the analysis.

REFERENCES

AMIN, M. S. (1955): Geological features of some mineral deposits in Egypt. Bull. Inst. Desert, Egypt, S. 1, 208–239.

BENCE, A. E. and ALBEE, A. L. (1968): Empirical correction factors of electron microanalysis of silicates and oxides. J. Geol. **67**, 382–403.

BÖHLKE, J. K. (1989): Comparison of metasomatic reactions between a common CO_2-rich vein fluid and diverse wall rocks: Intensive variables, mass transfers, and Au mineralization at Alleghany, California. Econ. Geol., **84**, 291–327.

CATHELINEAU, M. and NIEVA, D. (1985): A chlorite solid solution geothermometer. The los Azufres geothermal system (Mexico). Contrib. Mineral. Ret. **91**, 235–244.

CATHELINEAU, M.; BOIRON, M. C.; HOLLIGER, P.; MARION, P. and DENIS, M. (1988): Gold in arsenopyrite: Crystal chemistry, location and state, pysical and chemical conditions of deposition. Econ. Geol. mono 6: The geology of gold deposits, 328–341.

COLVINE, A. C.; ANDREWS, A. J.; CHERRY, M. E.; DUROCHER, M. E.; FYON, A. J.; LAVINGNE, M. J.; MACDONALD, A. J.; MARMONT, S.; POULSEN, K. H.; SPRINGER, J. S.; and TROOP, D. G. (1984): An integrated model for the origin of Archean lode gold deposits. Ontario Geol. Survey open-file rept., 5524, 98pp.

DEER, T. G.; HOCKES, A. H. and ZUSSMAN, M. M. (1985): An introduction to mineralogy. London, Academic Press, 307pp.

EL-MAHALLAWI, M. (1984): Petrology and geochemistry of the intrusive rocks of Umm Rus area, Central Eastern Desert, Egypt. Ph. D. thesis, El-Minya Univ., Egypt.

EL-RAMLY, M.; IVANOV, S. S.; KOCHIN, G. G. and others (1970): The occurrence of gold in the Eastern Desert of Egypt. In: Studies on some mineral deposits of Egypt. (Ed. by Moharram O. et al.). Geol. Surv. Egypt, part 1, section A, Artical no. 4, 53–64.

FOSTER, M. D. (1962): Interpretation of the composition and a classification of the chlorites. U. S. Geol. Surv. Prof. Paper 414 A, 1–33.

GROVES, D. I. and PHILLIPS, G. N. (1987): The genesis and tectonic control on Arcean gold deposits of the Western Australian Shield – a metamorphic replacement model: Ore Geology Rev. 2, 287–322.

HARRAZ, H. Z. and EL-DAHHAR, M. A. (1994): Fluid-wall rock interaction and its implication on gold mineralization at Umm Rus gold mine area, Eastern Desert, Egypt. J. Geol., Egypt. 38, 2, 713–747.

HARTMAN, G. AND WEDEPOHL, K. H. (1993): The composition of peridotite tectonites from the Ivreacomplex (N Italy), residues from melt extraction. Geoch. Cosm. Acta. **57**, 1761–1782.

HUME, W. F. (1937): Geology of Egypt. The minerals of economic value associated with the intrusive Precambrian igneous rocks. Geol. Surv. Egypt. V. II, part III, 805 pp.

KABESH, M. L.; HILMY, M. E. and BISHADY, A. M. (1967): Geology of the basement rocks in the area around Umm Rus gold mine, Eastern Desert, Egypt. J. Geol. Egypt **11**, 59–85.

KAMEL, O. A., EL MAHALLAWI, M. and HILMY, H. M. (1992): Mineralogy of the Umm Rus gold-bearing quartz veins and the surrounding alteration zones, J. Min. Soc. Egypt **4**, 55–86.

LEAKE, B. E. (1978): Nomenclature of amphiboles. Can. Miner. **16**, 501–520.

MACLEAN, W. H. and KRANIDIOTIS, P. (1987): Immobile elements as monitors of mass transfer in hydrothermal alteration: Phels Dodge massive sulphide deposit, Matagami-Quebec. Econ. Geol. **82**, 951–962.

MÜCKE, A. and ADJIMAH, K. (1994): Ore texture and paragenesis of the gold deposits of Prestea and Obuasi, Ashanti Belt, Ghana. An ore microscopic study. Geol. Jb D100, Hannover 163–195.

SABET, A. H. (1961): Geology and mineral deposits of Gebel El-Sibai area, Red Sea Hills, Egypt, U.A.R. Ph.D. thesis, Lieden State Univ. Netherland, 189pp.

SAUNDERS, C. M. and TUACH, J. (1991): Potassic and Sodic alteration accompaning gold mineralization in the Ratting Brook deposit, Western White Bay, New Foundland Appalachians. Econ. Geol. 86, 555–569.

STRUNZ, H. (1966): Mineralogische tabellen. Berlin-Germany, Röder and Leipzig, 560 p.

TAKLA, M. A. (1971): Ore mineralogical and geochemical studies of some basic and associated ultrabasic igneous rocks, Eastern Desert, Egypt. Ph.D. Thesis, Cairo Univ. Egypt.

Manuscript received 3 January, 1996.